

The Updated GEO Population for ORDEM 3.1

A. Manis⁽¹⁾, M. Matney⁽²⁾, P. Anz-Meador⁽³⁾, and H. Cowardin⁽³⁾

⁽¹⁾ HX5 – Jacobs JETS Contract, NASA Johnson Space Center, Mail Code XI5-9E, 2101 NASA Parkway, Houston, TX 77058, USA, alyssa.p.manis@nasa.gov

⁽²⁾ NASA Johnson Space Center, Mail Code XI5-9E, 2101 NASA Parkway, Houston, TX 77058, USA

⁽³⁾ Jacobs, NASA Johnson Space Center, Mail Code XI5-9E, 2101 NASA Parkway, Houston, TX 77058, USA

ABSTRACT

The limited availability of data for satellite fragmentations and debris in the geosynchronous orbit (GEO) region creates challenges to building accurate models for the orbital debris environment at such altitudes. Updated methods to properly incorporate and extrapolate measurement data have become a cornerstone of the GEO component in the newest version of the NASA Orbital Debris Engineering Model (ORDEM), ORDEM 3.1. For the GEO region, the Space Surveillance Network (SSN) catalog provides coverage down to a limit of approximately 1 m. A more statistically complete representation of the GEO population for smaller objects, which can pose a high risk to operational spacecraft, is thus dependent on dedicated observations by instruments optimized to observe debris smaller than the SSN cataloging threshold. For ORDEM 3.1, optical data from the Michigan Orbital DEbris Survey Telescope (MODEST) provided the input for building the GEO population down to approximately 30 cm (converting absolute magnitude to size). For smaller sizes, the size distribution of debris in the MODEST dataset was extrapolated down to 10 cm, and orbital parameters were estimated based on the orbits of the larger objects.

When compared to previous versions of the model, significant improvements were made to the process of building the GEO population in ORDEM 3.1, both in the assessment of fragmentation debris in the data and assignment of orbital elements within the model. A so-called “debris ring filter,” based on a range of angles between an orbit’s angular momentum vector and that of the stable Laplace plane, was applied to the data to reduce biases from non-GEO objects, such as objects in a GEO-transfer orbit. In addition, a new approach was implemented to assign non-circular mean motions and eccentricities to the fragmentation debris observed by MODEST because the short observation window (5 min) in GEO limits orbit resolution to a circular orbit assumption for assigning orbital parameters. For ORDEM 3.1, non-circular orbital elements were assigned using relationships that were identified between mean motion and the angle between the orbit plane and the stable Laplace plane, as well as between mean motion and eccentricity, based on breakup clouds modeled by the NASA Standard Breakup Model. This approach has yielded a high-fidelity GEO model that has been validated with data from more recent MODEST observation campaigns.

1 INTRODUCTION

The NASA Orbital Debris Program Office (ODPO) began development of the Orbital Debris Engineering Model (ORDEM) in the mid-1980s in support of the Space Station Program Office [1]. Initial manifestations of the model included analytical solutions representing the debris environment [2]. ORDEM96 was the first model that required a personal computer for effective implementation and pioneered the use of debris population ensembles characterized by altitude, eccentricity, inclination, and size [3]. ORDEM2000 replaced the curve fitting approach with a finite element representation of the debris environment [4]. ORDEM 3.0 represented a significant upgrade in terms of model features and capabilities. It extended the model to the geosynchronous orbit (GEO) region (up to 40,000 km), which enabled assessment of the orbital debris environment affecting circular to highly elliptical orbits, and implemented material density distributions as well as uncertainties for orbital debris fluxes [5]. The current version of the model, ORDEM 3.1, includes the same capabilities as its predecessor ORDEM 3.0, but updates the model populations using the most recent and highest-fidelity datasets from radar, *in situ*, and optical sources as well as new analysis techniques.

The Space Surveillance Network (SSN) catalog provides the fundamental dataset for ODPO modeling efforts. The SSN catalog is considered nearly complete for objects down to approximately 10 cm in low Earth orbit (LEO) and

1 m in GEO. To create a more statistically complete GEO population for ORDEM down to 10 cm in size, observations of GEO objects from the Michigan Orbital Debris Survey Telescope (MODEST) were used. Data from two observation periods covering 2004-2006 [6] and 2007-2009 [7] were used for ORDEM 3.1 development, and an additional dataset covering 2013-2014 was used for validation. Several new analysis techniques were employed in building the GEO component of ORDEM 3.1, including applying a so-called “debris ring filter” to best extract GEO fragmentation debris from the MODEST datasets. Also, new methods were utilized to assign more realistic orbits to MODEST targets based on correlations determined from modeled GEO breakups between mean motion (MM), eccentricity (ECC), and the angle between an object’s orbit and the stable Laplace plane. Lastly, two simulated breakups, potentially corresponding to unidentified breakups that occurred during the 2009-2013 break between MODEST observation campaigns, were added to the model to better match the MODEST 2013-2014 dataset.

This paper discusses the approach used to build the GEO population in ORDEM 3.1 in Section 2 and model validation results in Section 3. A summary is given in Section 4.

2 BUILDING THE STATISTICAL GEO POPULATION

2.1 REFERENCE POPULATION

The background population for ORDEM 3.1 is based on the SSN catalog. Cataloged objects are inserted into the environment via ODPO-maintained space traffic files and propagated forward in time using the NASA LEO-to-GEO Environment Debris (LEGEND) Model [8]. Fragments from known historical breakup events are created using the NASA Standard Satellite Breakup Model (SSBM), which describes the size, area-to-mass ratio, and velocity distributions of the breakup fragments [9]. Future populations were generated as the average of 100 Monte Carlo (MC) simulations, and future explosion and collision events were assessed probabilistically. For GEO, the LEGEND historical period covered 1957-2015, and the launch traffic for the years 2008-2015 was repeated every 8 years for the future propagation.

Fragmentation debris in GEO is implicitly included in ORDEM from the optical observations, so fragments from known historical breakups (i.e., prior to 2015) were excluded from the LEGEND reference population. As of the date of ORDEM 3.1 development, seven breakups had been confirmed in GEO [10] (see Table 1). Four of these breakups occurred during the historical period covered by LEGEND, two of which – the Ekran 2 spacecraft and Titan 3C (1968-081E) rocket body – were fully identified in terms of time and/or orbital elements at the time of the event. Two additional breakups – Ekran 4 and Ekran 9 – were recently confirmed by day of event only, with no breakup time or orbital element information available. Three GEO breakups occurred in 2016 or later, during the future projection of LEGEND, and were explicitly modeled in LEGEND using the NASA SSBM.

Table 1. Confirmed breakup events in GEO as of the time of ORDEM 3.1 development.

Satellite Name	International Designator	SSN Catalog Number	Launch Date	Breakup Date
Titan 3C Transtage R/B (OV2-5 R/B)	1968-081E	3432	26 Sep 1968	21 Feb 1992
Ekran 2	1977-092A	10365	20 Sep 1977	23 Jun 1978
Ekran 4	1979-087A	11561	03 Oct 1979	23 Apr 1981
Ekran 9	1982-093A	13554	16 Sep 1982	23 Dec 1983
Breeze-M R/B (Cosmos 2513 R/B)	2015-075B	41122	13 Dec 2015	16 Jan 2016
BeiDou G2	2009-018A	34779	14 Apr 2009	29 Jun 2016
Titan 3C Transtage R/B (OPS 0757 [TACSAT] R/B)	1969-013B	3692	9 Feb 1969	28 Feb 2018

2.2 SUPPORTING DATA

From 2001 to 2014, MODEST served as NASA’s primary optical detector for statistically surveying the GEO region to provide estimates of the number of detected objects as input for building the ORDEM GEO populations. MODEST is a 0.6-m aperture, Curtis-Schmidt of classical design and is located at the Cerro Tololo Inter-American

Observatory (CTIO) in Chile. The standard exposure time is 5 sec, with a total time between exposures of 37.9 sec. Detected objects that are found to be in the publicly-available SSN catalog, with available Two Line Elements (TLEs), are termed correlated targets (CTs). Detected objects not correlated to objects in the catalog are termed uncorrelated targets (UCTs). An object's instrumental magnitude is the direct observable in the MODEST survey dataset. Using an assumed range, r , of 36,000 km and a Lambertian phase function correction for an astronomical red "R" filter, the instrumental magnitude is converted to an absolute magnitude, $M_{abs}(R)$. Size, d , of each target is inferred from its absolute magnitude through the equation [11]:

$$d = \frac{2 \cdot r}{[\pi \cdot A_g \cdot \Psi(\alpha)]^{0.5}} \cdot 10^{\left[\frac{M_{abs}(R) + M_{sun}(R)}{-5.0}\right]} \quad (1)$$

where A_g is the given geometrical albedo of the object's surface, $\Psi(\alpha)$ is the phase function that defines how sunlight is scattered by the surface in a direction α to the observer, and $M_{sun}(R) = -27.103$ is the magnitude of the sun. Here, an albedo of 0.175 [12] and a diffuse Lambertian phase function at a phase angle of $\alpha = 0^\circ$ are used.

Absolute magnitude and size are inversely related so that low magnitude (bright) objects have a large size, and high magnitude (dim) objects have a smaller size. Fig. 1 shows the distribution in absolute magnitude for the 2004-2006 and 2007-2009 MODEST datasets. The MODEST system is capable of detecting 19th magnitude objects, which corresponds to approximately 10 cm in size given Eq. (1; however, note that the dataset is not complete to that magnitude (size). There are two peaks in the distribution, corresponding to CTs at lower magnitudes (larger sizes) and UCTs at higher magnitudes (smaller sizes). The peak around 12th magnitude (approximately 2.5 m) in both datasets corresponds to nonfunctional (and presumably tumbling) CTs, while functional CTs peak at around 10th magnitude [6, 7]. The MODEST datasets exhibit a roll-off in the absolute magnitude distribution for magnitudes greater than ~17 (smaller than ~30 cm), as seen in Fig. 1. This roll-off in the distribution reflects the detection capability of MODEST, not the true nature of the population. The true debris population is believed to continue at the same slope through fainter magnitudes (smaller sizes) based on comparisons with the standard breakup model for explosions (shown by the "NASA SSBM power law fit" dashed line in Fig. 1, scaled to approximately match the two MODEST datasets). Each MODEST detection has an assigned statistical weight, W , representing how many times that target should be counted for a statistical sampling of the population. The weight, or number of objects represented by each target in the MODEST dataset, statistically accounts for multiple detections of the same object as well as objects that are sampled from a population which is, on average, undetected or under-sampled.

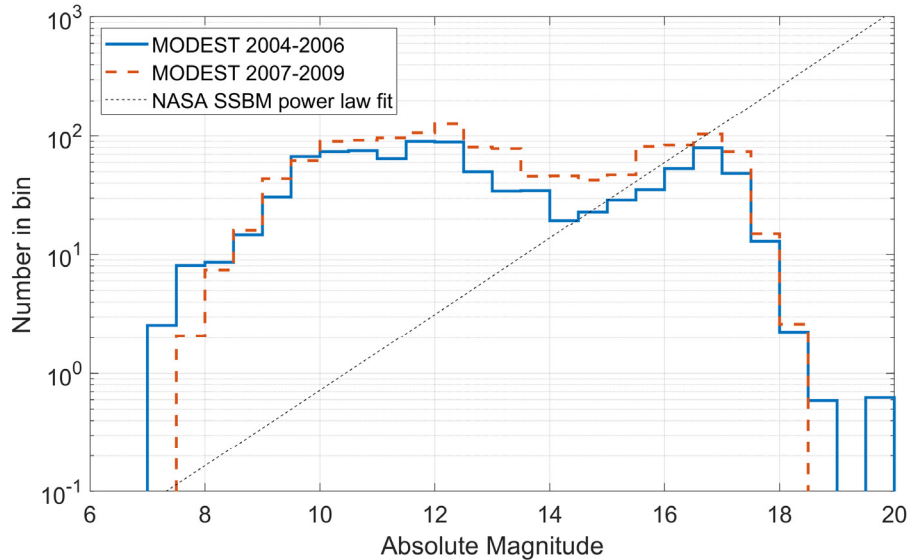


Fig. 1. Absolute magnitude distribution of the MODEST 2004-2006 and 2007-2009 datasets. The slope of the NASA SSBM power law for explosions, scaled to the MODEST distributions, is overlaid for reference.

Since each MODEST dataset is an independent set of statistical observations of the GEO debris environment, and the observed orbital elements for each MODEST target correspond to a specific detection date and time, the 2004-

2006 and 2007-2009 datasets were combined into a composite 2004-2009 dataset to build the ORDEM 3.1 GEO population. Each target in the datasets was propagated forward or backward in time to a common epoch of 0h UT 1 January 2007, corresponding roughly to the midpoint of the two datasets. The 2007-2009 dataset exhibits better coverage in circular mean motion (MM_{circ}) as compared to the 2004-2006 dataset, so a composite weight, W_{comp} , was assigned to each detection based on the observed MM_{circ} and given the completeness of each dataset, as summarized in Table 2. All subsequent references to weight or number of objects refer to the sum of the composite weights of individual targets, and the final model populations determined from the MODEST dataset take this weighting into account.

Table 2: Completeness in circular mean motion and composite weights calculated for the 2004-2006 and 2007-2009 MODEST datasets.

MODEST dataset	Mean Motion (MM_{circ} , rev/day)	Composite Weight
2004 – 2006	$0.9 \leq MM_{\text{circ}} \leq 1.15$	$W_{\text{comp}} = 0.5 \cdot W$
2007 – 2009	$0.7 \leq MM_{\text{circ}} \leq 1.3$	$W_{\text{comp}} = \begin{cases} 0.5 \cdot W, & 0.9 \leq MM_{\text{circ}} \leq 1.15 \\ W, & \text{otherwise} \end{cases}$

2.3 FRAGMENTATION DEBRIS FILTER

Only MODEST debris targets are of interest for building the statistical debris population smaller than the detection limit of the SSN catalog; larger, intact objects are included in the cataloged population modeled by LEGEND. However, extracting fragmentation debris from the MODEST datasets requires some careful analysis of the UCTs. While debris are identified in the CT portion of the database, the UCTs may contain debris as well as intact objects, but the focus for ORDEM development is on the smaller (fainter) UCTs, which are most likely to be debris. In addition, an object's inclination (INC) and right ascension of the ascending node (RAAN) can provide information on the object's orbit characteristics to designate it as most likely debris. Uncontrolled objects in GEO naturally precess in inclination / right ascension space due to effects from the Earth's oblateness and the gravity of the Sun and Moon [6]. This natural precession appears as a loop in the Cartesian coordinates of ($INC \cdot \cos(RAAN)$, $INC \cdot \sin(RAAN)$), termed the debris ring, which represents the projection of the orbit's angular momentum vector on the equatorial plane. Thus, controlled, intact objects will tend to clump near $(0^\circ, 0^\circ)$ in these coordinates, while derelict intact satellites and debris will tend to spread out in this ring. The ring of precession exhibits an approximately 50-year cycle, so that the location of a group of fragments around the ring can help identify the approximate time and location of the initial breakup event. Therefore, a method to filter UCTs for only those objects most likely to be GEO fragmentation debris was developed based on a target's size (magnitude) and location relative to this ring of uncontrolled fragmentation debris.

Using the albedo to size conversion assumptions discussed above (Eq. (1)), a size range limit of 30 cm – 1.25 m was imposed as a first-order filter for extracting fragmentation debris from the MODEST UCTs. The lower size limit of 30 cm corresponds to an upper limit in absolute magnitudes of approximately 17.1, which is consistent with the roll-off seen in Fig. 1 for smaller sizes (higher magnitudes) as well as typical reports of the completeness limit of the MODEST datasets. The upper size limit of 1.25 m approximately corresponds to a lower limit in absolute magnitude of 14.1, which is near the transition between the peaks for CTs and UCTs seen in the absolute magnitude distribution (Fig. 1). UCTs with lower absolute magnitudes (and larger sizes) are likely to be intact objects, so they were excluded to avoid over-counting objects already modeled in LEGEND. CT fragmentation debris was also included, regardless of size.

A new method was developed for filtering the MODEST datasets for fragmentation debris in an effort to exclude potential non-GEO objects, in particular objects in GEO-transfer orbits (GTO), which have highly elliptical orbits. Due to the short-time arc (5 min) for GEO observations and the circular orbit assumption, some non-GEO objects can appear in the rate box of a GEO object and would be misclassified as part of the GEO population. To screen for these, a debris ring filter was applied to best capture the ring of naturally precessing, uncontrolled GEO objects. Specifically, this filter was defined based on a range of angles between an object's angular momentum vector and a unit vector perpendicular to the stable Laplace plane, assumed to be inclined at 7.2° [13]. The angular momentum vector for a target's orbit is dependent on the target's identified INC and RAAN, and these orbital parameters are not largely affected by the circular orbit assumption.

The specific angular momentum unit vector, \hat{h} , of a generic orbit plane is given by:

$$\hat{h} = \hat{x} \sin(INC) \sin(RAAN) - \hat{y} \sin(INC) \cos(RAAN) + \hat{z} \cos(INC). \quad (2)$$

The specific angular momentum unit vector, \widehat{h}_0 , of an orbit coincident with the Laplace plane is then defined by:

$$\widehat{h}_0 = -\widehat{y} \sin(7.2^\circ) + \widehat{z} \cos(7.2^\circ). \quad (3)$$

The orbit angle, β , between an object's orbit plane and the stable Laplace plane is thus given by the dot product of the angular momentum vectors:

$$\beta = \cos^{-1}(\widehat{h} \cdot \widehat{h}_0). \quad (4)$$

The debris ring filter was defined by $\beta \in 7.2^\circ \pm \Delta$, with $\Delta = 2.6^\circ$ chosen to best capture the cluster of MODEST detections near the Titan 3C (1968-081E) breakup. Fig. 2 shows the UCTs and CT debris from the MODEST 2004-2009 composite dataset with size 30 cm – 1.25 m, projected in (INC·cos(RAAN), INC·sin(RAAN)) Cartesian space and overlaid with the limits of this debris ring filter. Clouds associated with the four GEO breakups that occurred prior to 2009 are also indicated.

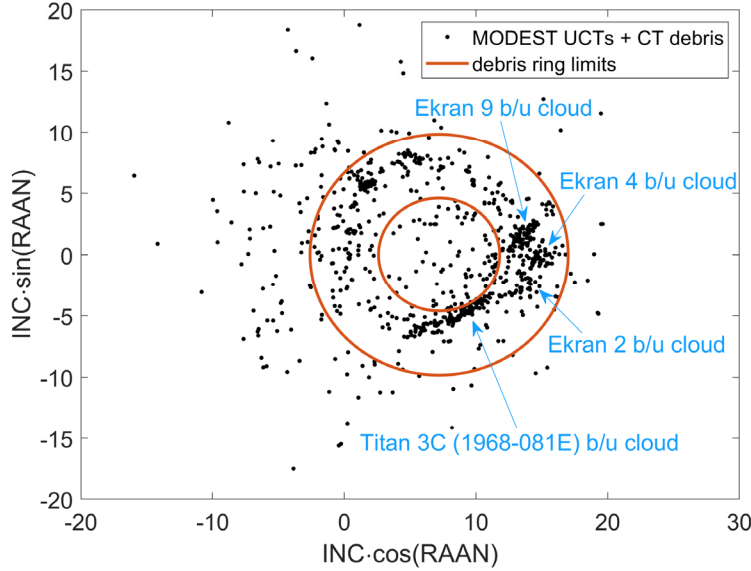


Fig. 2: MODEST 2004-2009 UCTs and CT debris with size 30 cm – 1.25 m in, projected in (INC·cos(RAAN), INC·sin(RAAN)) Cartesian space and overlaid with the debris ring filter limits. General regions of fragments from the four GEO breakups that occurred prior to the MODEST campaigns are indicated for reference. Objects seen outside the ring were excluded from the model as probable non-GEO objects imitating GEO behavior over the short-time arc of observations.

2.4 ASSIGNING ORBITAL ELEMENTS

Since a circular orbit assumption is made for MODEST UCTs, a more statistically accurate orbit was determined in order to better incorporate the MODEST targets into the ORDEM 3.1 GEO population. Specifically, a non-circular MM and non-zero ECC was assigned to each UCT based on breakups modeled using the SSBM. From the modeled breakups, correlations can be seen between MM and the orbit angle (β) as well as between ECC and MM. Fig. 3 and Fig. 4 show these relationships for the modeled Ekran 2, Titan 3C (1968-081E), Ekran 4, and Ekran 9 breakup clouds. Since currently there is no information available for the breakup time of day for Ekran 4 and Ekran 9, sample breakup times were used to model the breakups and propagate them to the common epoch of 0h UT 1 January 2007. The resulting sample breakup clouds were compared to the shapes of clusters in the MODEST composite dataset to visually determine a best-match for the estimated breakup time, leading to breakup times of 00:00 and 18:00 for the Ekran 4 and Ekran 9 breakups, respectively, on their respective breakup dates.

A MODEST target's orbit angle can be determined directly from the observed INC and RAAN, which are not strongly affected by the circular orbit assumption. Thus, the orbit angle was used first to assign a non-circular MM for the MODEST UCTs based on fits to the MM vs. β curves for each breakup. Then, a non-zero ECC was assigned based on fits to the ECC vs. MM curves. The exact curve fit for each modeled breakup cloud was assumed to represent the mean of a normal distribution from which to draw a random MM or ECC for a given value of α or

MM, respectively. The standard deviation for the normal distribution was calculated as twice the mean of the residuals of the curve fit. The regions around each identified breakup in $(INC \cdot \cos(RAAN), INC \cdot \sin(RAAN))$ space were used to identify which modeled curve fit to apply for a given MODEST UCT, e.g., if a MODEST UCT was located in a region around the Ekran 2 modeled breakup region then the Ekran 2 curve fit was applied. For a UCT not in a region near any of the identified breakups, MM and ECC were assigned based on curve fits for ECC vs. MM from a set of generic GEO breakups modeled with $MM = 0.99$ rev/day, corresponding to the peak in the mean motion distribution seen for cataloged GEO objects.

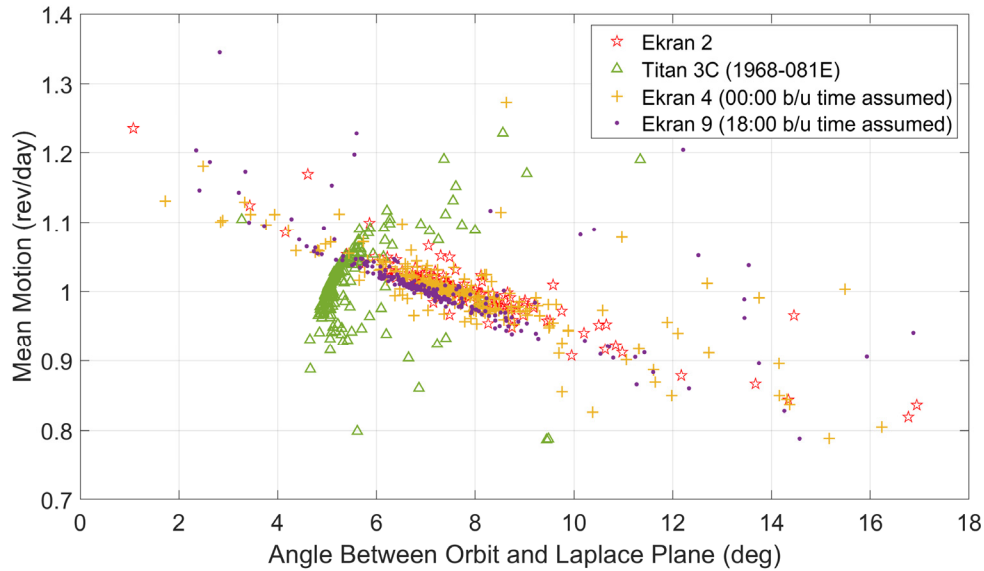


Fig. 3: Mean motion as a function of the angle between the orbit plane and the stable Laplace plane for the modeled Ekran 2, 4, and 9 and Titan 3C (1968-081E) breakup clouds.

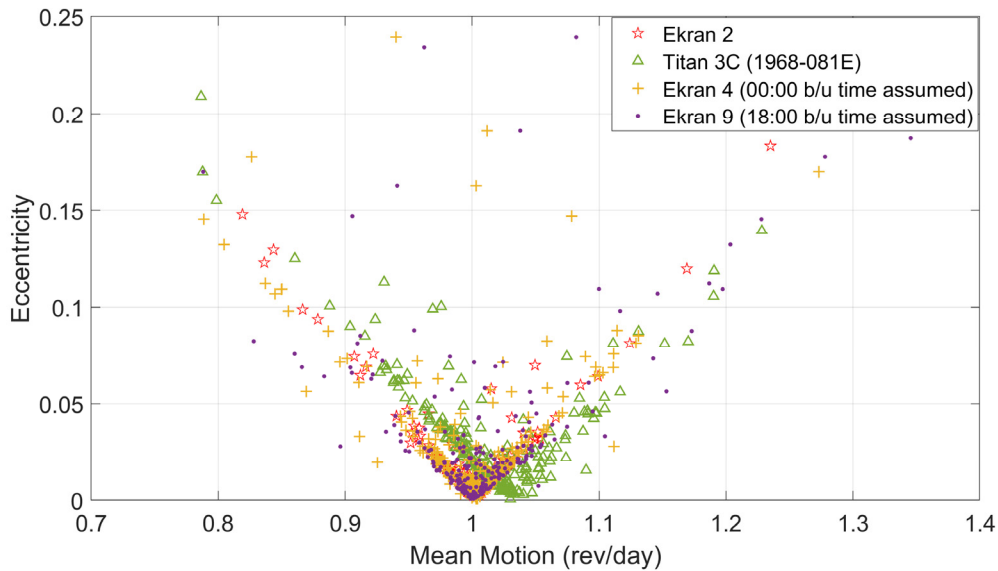


Fig. 4: Eccentricity as a function of mean motion for the modeled Ekran 2, 4, and 9 and Titan 3C (1968-081E) breakup clouds.

Since a circular orbit is assumed for each UCT in the MODEST datasets, the distributions in MM_{circ} for the resulting model and the MODEST dataset were compared to verify that the non-circular orbits assigned to the UCTs were statistically reasonable. For each non-circular orbit assigned to the UCTs, the range of possible MM_{circ} values the telescope might be expected to see from a particular non-circular MM and ECC orbit was computed. That is, using

an object's modeled MM and ECC, 100 samples of the velocity through the telescope field of view were calculated, and those values were converted into a corresponding value for MM_{circ} . The resulting MM_{circ} distribution is shown in Fig. 5 compared to that of the MODEST composite dataset. The number of objects in each bin is the sum of the composite weights of the objects in that bin. Uncertainties shown for the MODEST data points are the one σ confidence intervals from the standard Poisson counting error:

$$\sigma = \sqrt{\sum_{i=1}^M W_{\text{comp}_i}^2} \quad (5)$$

where M is the number of MODEST targets in the bin of interest, and W_{comp_i} is the statistical composite weight of an individual detection. In general, the circular MM distribution of the ORDEM 3.1 population provides a match with the MODEST data within the one σ , and certainly two σ , uncertainty bounds. For MM below approximately 0.9 rev/day, where the model and the data diverge more prominently, it is possible that non-GEO objects are classified as GEO objects in the MODEST datasets, even with the debris ring filter that was applied. This discrepancy is an area of ongoing investigation, but given the large uncertainties on the MODEST data points, indicating low statistical sampling, the overall agreement between ORDEM 3.1 and the MODEST data is considered quite good.

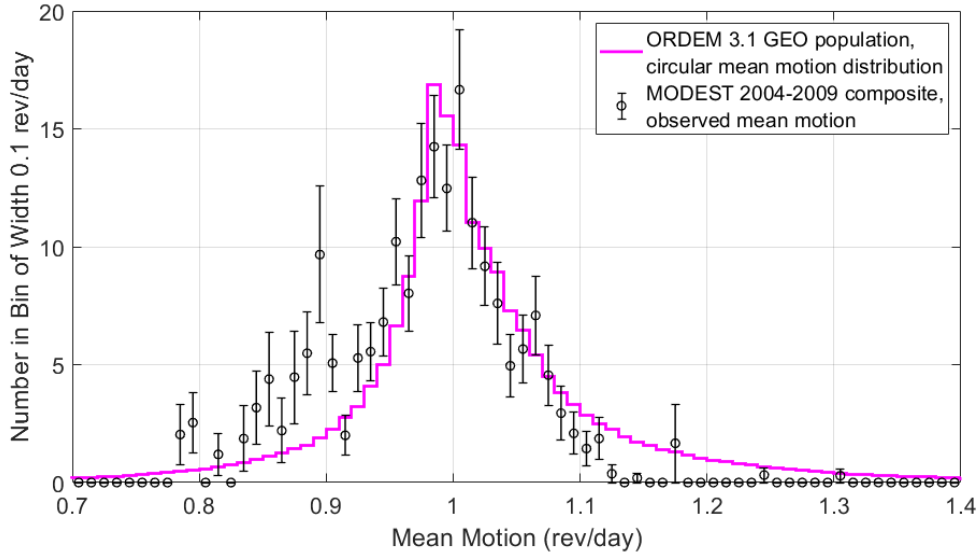


Fig. 5. Comparison of the mean motion distribution from ORDEM 3.1, converted to a predicted circular mean motion distribution, and the observed mean motion distribution from the MODEST 2004-2009 composite UCTs and CT debris.

2.5 EXTENDING THE MODEL TO 10 CM

The MODEST datasets are considered complete down to 30 cm, so the slope of the cumulative size distribution curve of the composite dataset was used to extrapolate the ORDEM 3.1 GEO population down to 10 cm. A power law fit was determined for the cumulative size distribution of the MODEST composite dataset, yielding the function:

$$N_C = 37.9L_C^{-1.6} \quad (6)$$

where N_C is the cumulative number of objects for a given size and larger, and L_C is the size (characteristic length) of the object. Note that the slope of this best-fit power law matches that of the NASA SSBM for explosions [9], which is in agreement with the expectation that explosions are more likely than collisions in GEO. The comparison of the binned differential size distribution of the MODEST composite dataset and the power law curve fit is shown in Fig. 6. Uncertainties shown for the MODEST data are the one σ confidence intervals from the standard Poisson counting error, as in Eqn. (5).

Following this power law, for each object expected in the 10 cm – 30 cm range, a size was assigned randomly from the cumulative power law curve in the same manner as is done for modeling breakups with the SSBM. An orbit was assigned randomly from the cumulative, normalized weight distribution of the composite dataset, defined by:

$$W_{cum_j} = \frac{\sum_{i=1}^j W_{comp_i}}{\sum_{i=1}^N W_{comp_i}}, \quad j = 1, \dots, N \quad (7)$$

where N is the total number of MODEST targets in the composite dataset. In this way, those targets with higher weights were more likely to be chosen. This approach intrinsically assumes that each object observed by MODEST is representative of a set of objects with the same orbit, originating from the same parent object, and introduces those fragments with a size too small to be detected by MODEST into the GEO population. To provide a statistical sample of the small GEO environment, 100 MC selections of non-circular orbits were assigned and each sample population was extended down to 10 cm based on the above approach.

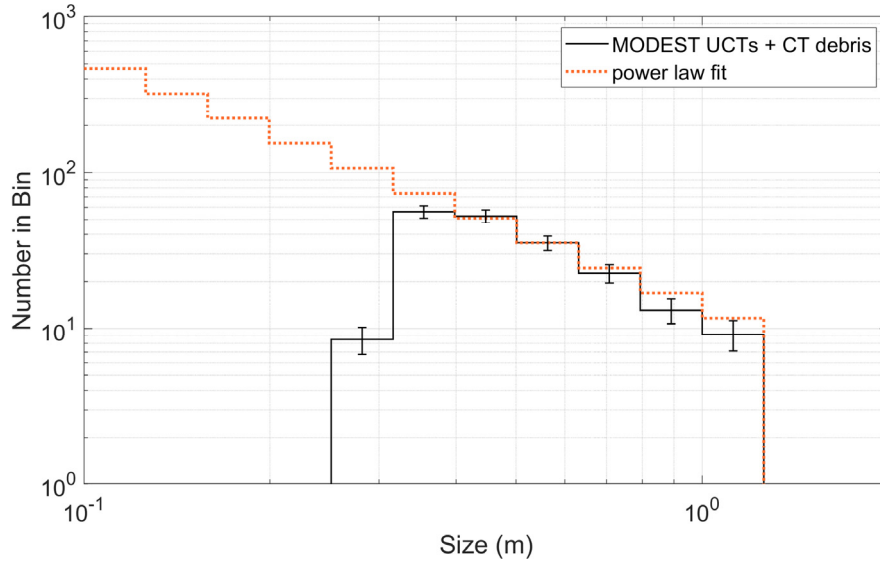


Fig. 6: Binned differential size distribution for the UCTs and CT debris from the 2004-2009 composite MODEST dataset. The distribution from the power law curve fit is shown extended down to 10 cm.

3 MODEL VALIDATION AND SIMULATED BREAKUPS

MODEST data from the 2013-2014 observation period, propagated to a common epoch of 0h UT 1 January 2014, were used to validate the ORDEM 3.1 GEO population. Comparisons in clock angle were performed between ORDEM 3.1 and the MODEST 2013-2014 data to ensure the model accurately represented the orbital evolution of the GEO debris population built from the 2004-2009 composite MODEST dataset. The clock angle is defined as an angle in the Cartesian coordinates of $(INC \cdot \cos(RAAN), INC \cdot \sin(RAAN))$ (see Fig. 2) where 0° is defined by a vector originating at $(7.2^\circ, 0^\circ)$ and pointing in the $(0^\circ, 0^\circ)$ direction, and the angle increases in a clockwise direction. Increasing clock angles thus represent the motion of uncontrolled objects around the debris ring, as discussed in Section 2.3.

Initial comparisons of the ORDEM 3.1 GEO population with MODEST 2013-2014 data showed more objects in the MODEST dataset in the clock angle ranges $0-60^\circ$ and $240-300^\circ$, as evident in Fig. 7 by the “ORDEM 3.1 initial GEO population” (dashed green) curve. This discrepancy suggests additional breakups occurred between 2009 and 2013, during the break between the MODEST observation campaigns used for building and validating ORDEM 3.1. It is not surprising that unidentified breakups would have occurred during this time period. Due to difficulties of observing small debris in GEO, fragmentation events are sometimes identified years after the event actually took place. For example, only four GEO breakups have been confirmed by the Combined Space Operations Center (CSpOC) as having occurred before the 2004 MODEST observations, and two of the events (Ekran 4 and Ekran 9) were identified to ODPO as breakups only recently, more than 30 years after the breakups actually occurred.

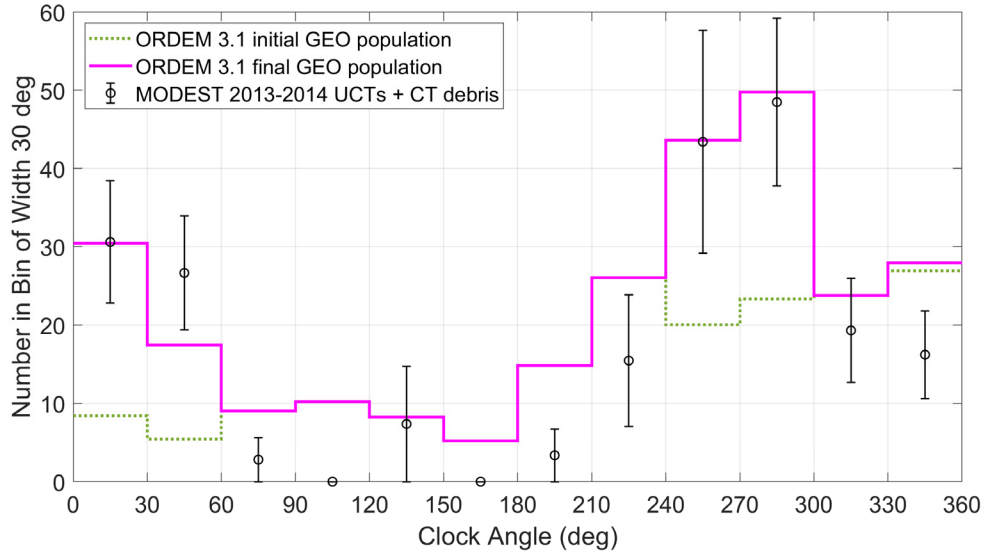


Fig. 7. Clock angle distribution of the ORDEM 3.1 initial GEO population, final GEO population including the addition of two simulated breakups, and MODEST 2013-2014 UCTs and CT debris, for sizes 30 cm – 1 m.

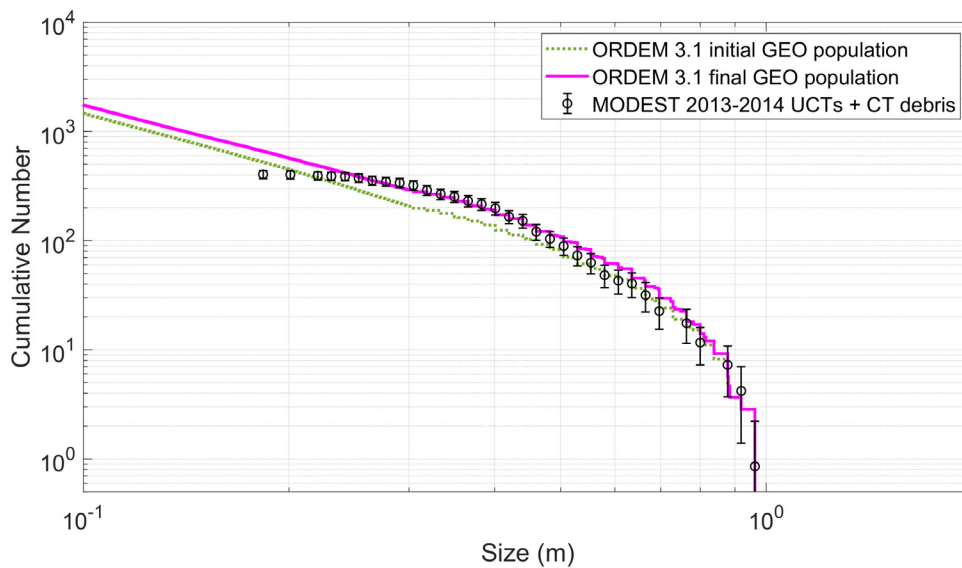


Fig. 8: Cumulative size distribution of the ORDEM 3.1 initial GEO population, final GEO population including the addition of two simulated breakups, and MODEST 2013-2014 UCTs and CT debris, for sizes 10 cm – 1 m.

To resolve the discrepancy between the GEO population developed from the 2004-2009 composite MODEST data and the later MODEST dataset, simulated breakups were added to the model. One breakup was added at the beginning of 2010 (0hr UT on 1 January 2010) to address the discrepancy in the clock angle range 0-60°. The “parent object” was assumed to have a mass of approximately 1900 kg, and the NASA SSBM was applied to model the breakup fragments. Through trial and error, a best match to the MODEST data was found by modeling the breakup with $INC = 0^\circ$, $RAAN = 0^\circ$, and mean longitude = 270° . An additional breakup was investigated to resolve the discrepancy between the model and the data in the 240-300° clock angle range. However, after an initial parametric investigation, a suitable breakup candidate time and orbit was not readily evident. While this is an area of ongoing investigation, for the purposes of ORDEM 3.1, fragments were added to the initial GEO population in this clock angle range to better match the data, and orbits were assigned to the extra fragments based on the objects in the MODEST 2013-2014 dataset with clock angle between 240° and 300°, similar to the method used for assigning non-circular orbital elements to UCTs discussed above. The final ORDEM 3.1 GEO population is shown by the solid magenta curve in Fig. 7. The model is clearly improved by the addition of the simulated breakups and is

generally within the one σ confidence intervals of the MODEST data. Overall, the comparison is a good match. An additional comparison of the ORDEM 3.1 GEO population to the MODEST 2013-2014 data in terms of cumulative size distribution of objects 10 cm – 1 m (see Fig. 8) also shows that addition of the two simulated breakups in the final GEO population yields a very good match to the MODEST data.

4 SUMMARY

The GEO population updated for the newest version of ORDEM incorporates several new analysis techniques to better characterize the GEO fragmentation debris environment based on MODEST data, which covers size ranges below the threshold of the SSN catalog. A debris ring filter was developed to better extract GEO fragmentation debris from the MODEST datasets based on the angle between an object's orbit and the Laplace plane. In addition, a new method was used to assign non-circular orbits to fragmentation debris using correlations between mean motion, eccentricity, and orbit angle seen in fragments from breakup clouds modeled for confirmed GEO breakups. Two artificial GEO breakups were added to provide a best match to the MODEST validation dataset in terms of clock angle and size distributions. The techniques discussed here have led to a high-fidelity GEO population in ORDEM 3.1 that matches the available MODEST data well.

5 REFERENCES

1. Kessler, D. J. "Orbital Debris Environment for Space Station," JSC Internal Note 20001, 1984.
2. Kessler, D. J., Reynolds, R. C., and Anz-Meador, P. D. "Orbital Debris Environment for Spacecraft Designed to Operate in Low Earth Orbit," NASA TM 100 471, 1989.
3. Kessler, D.J., Zhang, J., Matney, M.J., et al. "A Computer-Based Orbital Debris Environment Model for Spacecraft Design and Observation in Low Earth Orbit," NASA TM-104825, 1996.
4. Liou, J.-C., Matney, M., Anz-Meador, P.D., et al. "The New NASA Orbital Debris Engineering Model ORDEM2000," NASA/TP-2002-210780, 2002.
5. Stansbery, E.G., Matney, M.J., Krisko, P.H., et al. "NASA Orbital Debris Engineering Model ORDEM 3.0 – Verification and Validation," NASA/TP-2015-218592, October 2015.
6. Abercromby, K.J., Seitzer, P., Barker, E.S., et al. "Michigan Orbital DEbris Survey Telescope Observations of the Geosynchronous Orbital Debris Environment, Observing Years: 2004 – 2006," NASA/TP-2010-216129, August 2010.
7. Abercromby, K.J., Seitzer, P., Cowardin, H.M., et al. "Michigan Orbital DEbris Survey Telescope Observations of the Geosynchronous Orbital Debris Environment, Observing Years: 2007 – 2009," NASA/TP-2011-217350, September 2011.
8. Liou, J.-C., Hall, D. T., Krisko, P. H., and Opiela, J. N. LEGEND – A Three-Dimensional LEO-to-GEO Debris Evolutionary Model, *Adv. Space Res.*, Vol. 34, pp. 981-986, 2005.
9. Johnson, N.L., Krisko, P.H., Liou, J.-C., and Anz-Meador, P. NASA's New Breakup Model of EVOLVE 4.0, *Adv. Space Res.* Vol. 28, Issue 9, pp. 1377-1384, 2001.
10. Anz-Meador, P.D., Opiela, J.N., Shoots, D., and Liou, J.-C. "History of On-orbit Satellite Fragmentations (15th Edition)," NASA/TM-2018-2220037, 2018.
11. Barker, E.S., Africano, J. L., Hall, D. T., et al. Analysis of Working Assumptions in the Determination of Populations and Size Distributions of Orbital Debris from Optical Measurements. In *Proceedings of the 2004 AMOS Technical Conference*, Wailea, Maui, HI, pp. 225-235, 2004.
12. Mulrooney, M., Matney, M., and Barker, E. A New Bond Albedo for Performing Orbital Debris Brightness to Size Transformations, IAC-08.A6.2.7, 2008.
13. Rosengren, A.J., Scheeres, D.J., and McMahon, J.W. The Classical Laplace Plane as a Stable Disposal Orbit for Geostationary Satellites, *Adv. Space Res.*, Vol. 53, pp. 1219-1228, 2014.